Mechanism of the Hydrogen/Platinum(111) Fuel Cell†

L. Blum*

Department of Physics, P.O. Box 23343, University of Puerto Rico, Rio Piedras, PR 00931-3343

N. Marzari

Department of Materials Science, MIT, Cambridge, Massachusetts 02138

R. Car

Department of Chemistry, Princeton University, Princeton, New Jersey 08544

Received: June 28, 2004; In Final Form: August 24, 2004

We discuss our recently proposed mechanism for the electro-oxidation/reduction on Pt(111) surfaces (*J. Electroanal. Chem.* **2002**, *537*, 7) in the presence of sulfuric acid. The bisulfate ion has a large dipole moment and is strongly adsorbed on the positive electrode. Due to the large field gradients, the oxygen atoms of the adsorbed water molecules (and the dipoles) point down and bind to the on-top positions of the platinum substrate. As the electrode becomes more negative, the field gradient changes direction, and the water dipoles gradually reverse their orientation. At a certain critical value of the orientational parameter (which depends also on the bisulfate surface concentration), a two-dimensional honeycomb array of hydrogen bonded water molecules is formed. This is a new form of solid water, a true two-dimensional "ice". For these negative potentials, the stable structure has one of the hydrogen atoms of the water pointing down, and this means that it is adsorbed by the hollow site of the Pt lattice. To satisfy the stoichiometry of the hydrogen bonds, we need to adsorb one-third of the surface sites of H^+ ions. The following reversible reaction occurs: $(H_5O_2^+)_3 + 6e^- \rightleftharpoons 6H + (H_3O_2^-)_3$. For the (111) surface of platinum and because of the geometrical matchup (the Pt−Pt distance is 2.77 Å, and the water diameter is 2.76 Å) this reaction occurs as a first-order transition, visible in the voltammogram as a sharp peak. From the $[H^+]$ concentration dependence of this sharp spike, we get an effective charge of 1.02 ± 0.02 for the adsorbed moiety. High-accuracy quantum calculations on a five-layer platinum metal slab show that this compound is stable in the absence of bisulfate ions. The quantum calculations show also that the hydrogen atoms in the hollow positions are neutralized. Since there are two-thirds of the Pt sites in the hollow positions, our model gives a natural explanation to the well-known fact that the hydrogen yield is 2/3 on this surface. We have revised our theory to shift the turning point of the water molecules to the transition potential where the HER honeycomb phase is formed. The turning point is in general agreement with the recent laserinduced measurements of the potential of zero charge.

1. Introduction

The redox reaction of hydrogen on platinum electrodes is important to fuel cell technology. It was first studied by Clavilier et al. using his pioneering techniques of preparing monocrystalline electrode surfaces.[1,2] We have in recent years presented a molecular theory that accounts for most of the experimental observations.[3−6] In the present paper, we revise the parametrization of our previous work and show that our theory is also in accordance with recent measurements of the point of zero charge.

This system has been studied experimentally by a large number of authors.[2,7−26] The Clavilier voltammogram for the (111) surface is shown in Figure 1 on a rather perfect single crystal.[27] The major difference with previous voltammograms is the very sharp spike near 0.5 V (RHE), which clearly indicates a first-order phase transition. Recent concentration-dependence experiments[27] shown in Figure 2 demonstrate that the adsorbed species has electrovalence 1+. The only possibility is that a proton in some hydrated form is part of the reaction that forms the hydrogen electroreduction reaction (HER) compound, which is this new form of 2-dimensional ice.[3−6]

We know from the STM observations that in the region between 0.505 and 1.0 V, a structure of elongated hexagons with surface coverage $\theta = (1/5)$ exists.[28−31] It is known from ex situ experiments[32−34] that this structure corresponds to the formation of a water−bisulfate complex. From the statistical mechanics of hexagons and long hexagons developed by A. Coniglio,[35] we know that no order−disorder transitions are possible for elongated hexagons, which because of entanglements will only undergo a gradual glass transition between a disordered low density and a disordered high-density phase. The model of water chains between the adsorbed bisulfate ions[30−34] is more reasonable physically, although no sharp spikes in the voltammogram will occur, since this is a one-dimensional chain. However, in all of this work, the structure of the water chain is drawn with alternating orientation of the water molecules to keep the O−H−O bond from bending. The first observation is that even at room temperature, the proton is a quantum particle

† Part of the special issue "Frank H. Stillinger Festschrift".

10.1021/jp047188j CCC: $27.50
Published on Web 11/12/2004

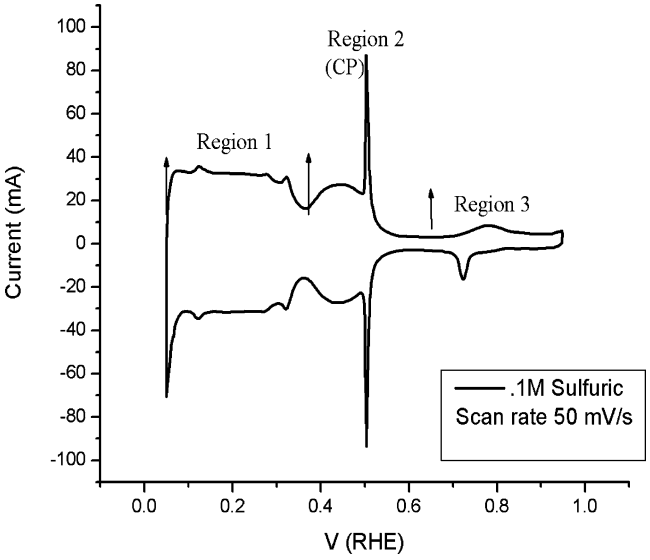

Figure 1. The voltammogram for the H_2/Pt(111)/SO_4H_2(0.1 M) system is divided into three regions: (1) the UPD region, (2) the CP butterfly region, and (3) the positive region.[27]

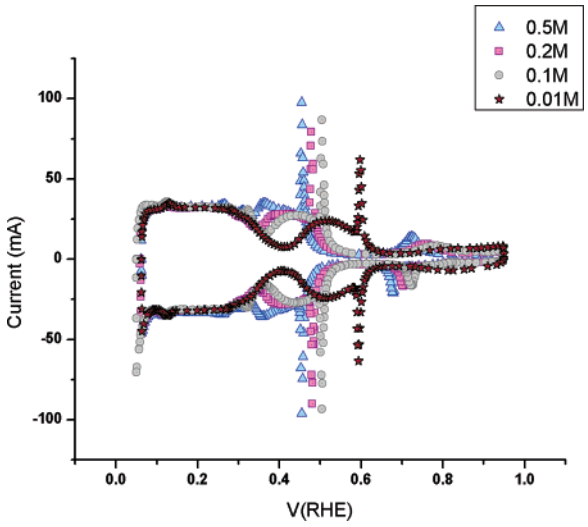

Figure 2. Voltammograms for the same system for 0.5, 0.2, 0.1, and 0.01 M solutions of sulfuric acid. Scan rate is 50 mV/s, as in Figure 1 (see ref 27).

and ,hence, appreciably delocalized. Neutron-scattering experiments have shown that even in regular ice, the O−H−O bond deviates considerably from the straight line.[36] In our model, we require that the water molecules are oriented the same way by the very strong field gradients at the electode interface, in accordance with observations made long ago by Mott and Watts-Tobin.[37] The second observation is that point charge models[38−41] yield very directional hydrogen bonds, which are never observed experimentally.[42] Diffraction experiments in water cannot observe angular dependencies much beyond the octupole. For that reason, we use an octupolar model of water,[43−45] which allows for considerable bending of the hydrogen bonds. Our discussion is centered around the voltammogram shown in Figure 1. In previous papers,[3−6] we have assumed that the hump observed around 0.6 V was due to the reorienting of the water molecules. It is more logical to place the turning point around the transition spike, which is what we do in the present work. This results in a turning point that is in agreement with the recent experiments[27] but leaves the theory of region 3 (Figure 1) unexplained, at least for the time being. The discussion of the origin of this hump will be left for a future paper.

For the region between 0 and 0.505 V (RHE) in Figure 1, there are no direct structural experiments, but there is compelling evidence that it must be an ordered phase. We propose a honeycomb 2-dimensional ice-like structure. The vertexes of the honeycomb are the oxygen atoms, and each one of them has a hydrogen directly below which sits in the hollow position of the (111) platinum surface. Those hydrogen atoms are the ones that get reduced to H° and are exactly 2/3 of the surface atoms.[1] We, thus, have for the first time a model that explains in a natural way this fact. The region between 0.5 and 0.35 V of Figure 1 shows a bulge that is known to be faradaic from the CO displacement experiments by Feliu et al.[11−13] Radiotracer experiments show that they correspond to the desorption of SO_4H^+.[18] The HER compound in our theory is this 2-dimensional ice phase, which is stable even in the absence of bisulfate.

The region between 0 and 0.35 V of Figure 1 corresponds to the discharge of the HER compound, $(H_5O_2^+)_3$, and undergoes the reaction

$$(H_5O_2^+)_3 + 6e \rightarrow 3H_2^+ (H_3O_2^-)_3 \qquad (1)$$

Density functional calculations of this reaction are presented in the last part of this paper. They show that both forms of the HER $(H_5O_2^+)_3$ and $(H_3O_2^-)_3$ are stable on the surface so that this reaction scheme is completely reversible.

In Section 2, we describe the basic ingredients of our theory, which we then use in Section 3 to describe the elementary steps in the reaction. In Section 4, we calculate the theoretical voltammogram and compare the result to experiment. Final comments are given in Section 5.

2. Basic Ingredients of the Theory

It is outright impossible to study the structure and transformations of any surface electrochemistry problem from first principles[46] without a reliable and manageable theory, which is needed to predict the structures and transformations of a given electrode reaction. Blum and Huckaby[47−49] developed such a theory and applied it to the UPD (under potential deposition) of Cu/Au (111)[50−52] very successfully: The structure and phase transformations of the UPD layer were correctly predicted before experimental verification.[53] [The structure first proposed by Blum et al.[52] is identical to that of Toney et al.[53] except for the O−Au distance: Toney's is longer by 1 Å. The vertical resolution of the Toney experiment is bigger than 1 Å.]

A simple but systematic approach is to divide the problem into two manageable problems:

1. The classical smooth electrode problem. We would calculate the charge and density profiles, as well as the interactions between particles near the electrode, as a function of the applied potential. For point charges in a continuum dielectric, this is the Gouy−Chapman problem.

2. The structured surface problem. We now consider a crystal surface which is represented by a collection of adsorption sites. The parameters of the adsorption isotherm are the contact density (i.e., the number of particles touching the surface) and the contact pair correlation function.

We use in our analysis an exact projection method that was first used in the mathematically exactly solvable model of a one-component plasma in two dimensions.[54] In this case, the interface was a line decorated with equally spaced adsorption sites, and no phase transformation occurs. This projection method was then extended to real electrode interfaces.[47,48] In

this theory, the parameters of the lattice-phase transition problem are rigorously derived from the correlations and density profiles from the smooth wall problem: The fugacity parameter is rigorously derived from the contact density of the smooth wall; the site−site interaction parameter, from the inhomogeneous pair correlation functions of the smooth wall problem. This is very different from just using phenomenological coefficients, since in our case, the parameters are clearly structural and derivable from specific models, which is what we are doing in this work.

The full Hamiltonian of the entire 3-dimensional system is projected onto an equivalent "electrode" surface lattice: this means that the adsorbed moieties interact through an effective potential in which all quantum, solvation, and double layer forces are included. For very dilute solutions, such as the one of our present example, the exponential (Poisson Boltzmann) approximation is asymptotically accurate.

2.1. Adsorption At Structured Interfaces. Our model of chemisorption on structured interfaces is the correct statistical mechanics formulation of the Langmuir−Frumkin model: The binding process of individual species is described by an adsorption site with a binding free energy or affinity. This generates a theory with a complete description of the cooperative effects that take place at the surface.[47,48] The total Hamiltonian is separated into two parts,

$$H = H_0 + H_S \tag{2}$$

H_0 is the Hamiltonian for the smooth wall electrode, while H_S represents the adsorption sites interaction, which are considered as points on the electrode surface with a certain specific affinity. The explicit form of this Hamiltonian is described, and the details of the calculations can be found in the references cited above.

Combining these expressions we arrive at the formal expression

$$Z/Z_0 = \sum_{n=0}^{N}\left(\frac{\lambda\rho_1{}^0(0)^n}{n!}\right)\sum_{\text{adsorption sites}} e^{-\beta\omega_n(\mathbf{R}_1,\mathbf{R}_2,...,\mathbf{R}_n)}$$

$$= \sum_{n=0}^{N}\frac{z^n}{/n!}\sum_{\text{adsorption sites}} g_n(\mathbf{R}_1, \mathbf{R}_2, ..., \mathbf{R}_n) \tag{3}$$

where the fugacity is

$$z \equiv z_i = \lambda\rho^0(0) = z_i(\psi) = z_i = \lambda_i(\psi)\rho_i^{\circ}(0, \psi) \tag{4}$$

λ_i is the affinity parameter, $\rho_i(0)$ is the contact density of component, and we understand that these quantities are all potentially ψ-dependent. g_n is the n particle correlation function for n ions sitting at positions($\mathbf{R}_1$, $\mathbf{R}_2$, ..., $\mathbf{R}_n$). The most relevant one is g_2, the pair correlation function.

$$g_2 = g_2^0(\mathbf{R}_i, \mathbf{R}_j) \quad [\text{i, j = nearest neighbors}] \tag{5}$$

The excess free energy is

$$\Delta f^s = \frac{-1}{\beta A}\ln(Z/Z_0) \tag{6}$$

where A is the area of the interface. We also deduce the fraction of occupied sites θ,[54]

$$\theta = -\frac{A\beta\lambda}{M}\frac{\partial\Delta f^s}{\partial\lambda} \tag{7}$$

where M is the number of adsorption sites on the electrode surface.

It has been shown that f^s(eq 6) in general and θ in particular can be written as a general fraction or Pade approximant.[48]

$$\theta = \frac{\mathcal{A}'(\mathbf{z})}{1 + \mathcal{A}(\mathbf{z})} \tag{8}$$

Here, $\mathcal{A}(\mathbf{z})$ is a generic notation for asymptotic clusters, which correspond to certain structures of adsorbed compounds.

In the simplest example, $\mathcal{A}(\mathbf{z})$ is

$$\mathcal{A}(\mathbf{z}) = z_i \tag{9}$$

and eq 8 becomes the Langmuir adsorption isotherm.

$$\theta = \frac{\lambda\rho_1{}^0(0)}{1 + \lambda\rho_1{}^0(0)} \tag{10}$$

The asymptotic behavior of $\mathcal{A}(\mathbf{z})$ is described by a few dominant structures, which depend on interaction parameters g_2, g_3, ..., and which are obtained from theory (for example, the cluster variation method).[55−58] The adsorption of species i on the platinum surface primarily depend on the activities of these adsorbates and the lateral interactions existing between them.[47,48,54]

The activity of a species i is given by the product between a sticky parameter $\lambda_i(\psi)$ and the species contact density at the surface $\rho_i^{\circ}(0,\psi)$, as

$$z_i = \lambda_i(\psi)\rho_i^{\circ}(0, \psi) \tag{11}$$

The sticky parameter $\lambda_i(\psi)$ is a parameter characterizing the quantum mechanical interaction between the adsorbate and surface and will be potential-dependent. We write[58]

$$\lambda_i(\psi) = \exp\{-\beta\kappa_i\zeta_i e(\psi - \psi_{\text{ref}})\} \tag{12}$$

where e is the elementary charge, ζ_i is the partial charge of the adsorbate at the surface, and κ_i is a binding constant characterizing the overlap of electron orbitals between the adsorbate and surface atoms. The actual values of the three parameters κ_i, ζ_i, and ψ_{ref} reflect the potential dependence of the adsorption parameter λ_i. In most cases, we can safely assume that this dependence is weak so that

$$\kappa_i, z_i \simeq 0 \tag{13}$$

The potential dependence of the contact density, $\rho_i^{\circ}(0, \psi)$, is given the BIMSA-EXP approximation,[59,60] which is asymptotically exact in the limit of zero concentration and infinite adsorption constant.

$$\rho_i^{\circ}(0, \psi) = \rho_i^{\circ}(0,0)\exp\{-\nu_i e\beta(\psi - \psi_{\text{pzc}})\} \tag{14}$$

Combining these two relations, we find the activity z_i is

$$z_i = \lambda_i(0)\rho_i^{\circ}(0, 0)\exp\{-\beta\gamma_i e(\psi - \psi_0)\} \tag{15}$$

where

$$\gamma_i = \nu_i + \kappa_i\zeta_i = \nu_i \tag{16}$$

Summarizing,

$$\nu_i = -\frac{\left(\frac{\kappa T}{e}\right)}{\left(\frac{dV}{d\log c}\right)} = -\frac{25.68\ \text{mV}}{\left(\frac{dV}{d\log c}\right)} \tag{17}$$

where $((dV/d\log c))$ is the slope of the peak position curve.

This relation has been verified for the electrodeposition of bulk copper on Au(111).[52] When the peak position is properly corrected for kinetic effects,[61] that is, we simply take

$$\psi_{\text{equilibrium}} = \frac{1}{2}\{\psi_{\text{oxidation}} + \psi_{\text{reduction}}\} \tag{18}$$

then the bulk deposition electrovalence is

$$\upsilon_{Cu} = 2.04 \tag{19}$$

and it should be 2.

Figures 2 and 3 show the results of an experiment in which the voltammogram was measured at four different concentrations of sulfuric acid. The concentration of hydrogen ions can be calculated using the BIMSA-EXP approximation:[60] Except for very dilute solutions, the dominant species is SO_4H^-, so we take

$$c_{SO_4H^-} \simeq c_{H^+}$$

with the result (no adjustable parameters!)

$$\nu = 1.02 \tag{20}$$

Using the BIMSA result,[60] which includes the dissociation reaction

$$SO_4H^- \rightleftharpoons SO_4^{2-}H^+ \tag{21}$$

however, yields the slightly higher value

$$\nu = 1.04 \tag{22}$$

as shown in Figure 3.

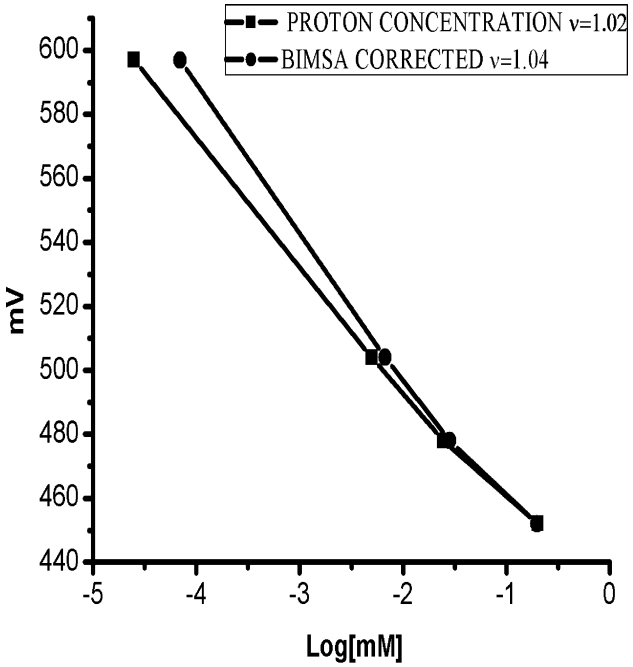

Figure 3. Electrovalence of the adsorbed ion from a change of the peak position as a function of concentration shown in Figure 2. The result is $\nu_i = 1.02$.

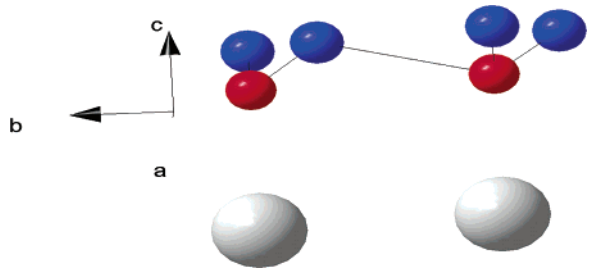

Figure 4. Structure of the hydrogen bond between two oxygen atoms that are directly bound to platinum atoms (larger gray spheres) at the surface of the electrode.

2.2. The Water Potential. The theory developed puts some severe constraints on the water model potential:

• It must be of tetrahedral coordination. Although the very first point-charge models used for liquid water were tetrahedral,[38,39] the currently most popular potentials[40,41] derive from the Bernal three-point charge model and are planar. Such models are inconsistent with the phase transformation proposed in this work, because the changes in orientation of the water molecule cannot produce the geometrical transition from the linear chain to a 2-dimensional honeycomb ice structure by adsorption of one-third of H^+.

• If all of the water molecules are oriented the same way and bound to the Pt, the angle O−H−O of the hydrogen bond will be bent. The angular part of the potential must be relatively soft. As was discussed in earlier work,[42] the experimental resolution of the angular part of the pair correlation function is limited by the neutron-scattering form factors, which are very small beyond the octupole−octupole term (spherical harmonic $l \geq 3$). Most of the current water potentials using point charges carry terms up to $l \simeq 8-12$, which cannot be measured.

The O−H−O bond is generally not straight in the few experiments in which it has actually been measured. In ice, it is close to 170°.[36] Keeping all the waters at the same distance from the Pt requires a flexible, tetrahedral water molecule, since the natural angle for a rigid tetrahedral structure would be 129°. Viewed from the two molecules participating in the hydrogen bond (see Figure 4), the distortion from the tetrahedral structure for one of the water molecules is 35°, while for the other it is only 15°. The most likely scenario, however, is that the Pt−O distances are not the same, so that the angular distortion is even smaller. The distortion from the Chidambaram structure is likely to be more like 30° and 10°. Detailed quantum mechanical calculations for the honeycomb HER compound[5] show that the hydrogen bonded structure is nearly perfectly flat.

There is another more fundamental limitation of the liquid state: In the invariant expansion of the molecular pair correlation function,[62] only the $\chi = 0$ representation contributes to the liquid scattering cross section.[42,62,63] The $\chi = 0$ is the average of the pair correlation functions around the intermolecular axis. This means that any structural features of the pair of molecules are averaged by smearing them around the intermolecular axis. In other words, the diffraction pattern will not distinguish between a planar and a tetrahedral molecular geometry. For our purposes, the Bernal-type flat models do not work.

• It must be analytical to include in the calculations explicitly the applied field effects and ion solvation:

2.2.1. Analytical Water Model. The analytical tetrahedral Yukagua model of water satisfies all of these requirements[44,45] and agrees very well with the structure of liquid water as

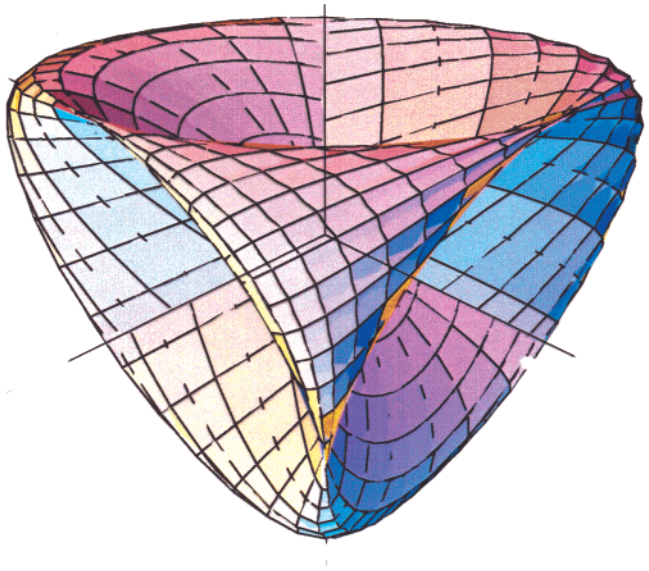

Figure 5. Octupole potential for water−water interactions.

measured by neutron diffraction[64] as well as a large number of properties of bulk water.[43−45,65−67] We summarize our previous results:

The explicit form of this potential is[45]

$$u(\mathbf{1},\mathbf{2}) = u^{\mathrm{SP}}(\mathbf{1},\mathbf{2}) + u^{\mathrm{D}}(\mathbf{1},\mathbf{2}) + u_0^{\mathrm{T}}(\mathbf{1},\mathbf{2}) \qquad (23)$$

where **1** represents the position and orientation of molecule 1 (or 2). The potential has three terms:

1. The short-range spherical part,

$$u^{\mathrm{SP}}(1,2) = \begin{cases} \infty & r_{12} < \sigma \\ \dfrac{K^{(00)}}{r_{12}} e^{[-z_1(r_{12}-r_c)]}[e^{[-z_2(r_{12}-r_c)]} - .2] & r_{12} > \sigma \end{cases} \qquad (24)$$

where r_{12} is the distance between the centers of molecules 1 and 2;

2. The electrostatic dipole interaction,

$$u^{\mathrm{D}}(\vec{1},\vec{2}) = \frac{1}{r_{12}^{3}}\left[\vec{\mu}_1\cdot\vec{\mu}_2 - 3\frac{(\vec{\mu}_1\cdot\mathbf{r}_{12})(\vec{\mu}_2\cdot\mathbf{r}_{12})}{r_{12}^{2}}\right] \qquad (25)$$

where $\vec{\mu}_i$ is the dipole moment of molecule i;

3. The tetrahedral term, which is expressed in terms of only the projections of the three director vectors $\vec{x}_i$, $\vec{y}_i$, $\vec{z}_i$, of each molecule on $\mathbf{r}_{ij}$,

$$\tau_i^{(x)} = [\vec{x}_i\cdot\mathbf{r}_{ij}]$$

$$\tau_i^{(y)} = [\vec{y}_i\cdot\mathbf{r}_{ij}]$$

$$\tau_i^{(z)} = [\vec{z}_i\cdot\mathbf{r}_{ij}] \qquad (26)$$

We form the angular function

$$\vartheta^{(\mathrm{oct})}(\mathrm{ij}) = \tau_i^{(z)}\{[\tau_i^{(x)}]^2 - [\tau_i^{(y)}]^2\} + \tau_j^{(z)}\{[\tau_j^{(x)}]^2 - [\tau_j^{(y)}]^2\} \qquad (27)$$

which represents the octupolar potential seen by the center of molecule 2 in the tetrahedral field of molecule 1. The shape is that of a tetrahedron with its faces carved in, as shown in Figure 5, clearly very soft in the angular bending modes. A term is added to account for the polarity of the hydrogen bond:

$$\vartheta^{(\mathrm{tetr})}(\mathrm{ij}) = \{2\tau_i^{(z)}\cos\theta_m + [\tau_i^{(x)}]^2 - [\tau_i^{(y)}]^2\}\{2\tau_j^{(z)}\cos\theta_m + [\tau_j^{(x)}]^2 - [\tau_j^{(y)}]^2\} \qquad (28)$$

Finally, we write

$$u^{\mathrm{T}}(\mathbf{1},\mathbf{2}) = K_{\mathrm{T}}e^{[-z_1(r_{12}-r_c)]}[a^{(03)}\vartheta^{(\mathrm{oct})}(12) + a^{(12)}\{\vartheta^{(\mathrm{tetr})}(12)\}] \qquad (29)$$

The parameters K_T, r_c, $a^{(03)}$, and $a^{(12)}$ were discussed in our previous work.[45]

The pair distribution functions obtained by Monte Carlo simulation using $K^{(00)} = 600$ KJ/mol, $r_c = 3.2$ Å, $z_1 = 5$, $z_2 = 15.5$, $a^{(03)} = 15$, and $a^{(12)} = 7$, with a dipole moment were taken as 2.25 D. As can be seen in Figures 6, 7, and 8, the agreement with the neutron diffraction experiments is good. The mean molar energy obtained in this way, -53.4 ± 0.7 kJ/mol, is higher than the experimental one of -42 kJ/mol.[45] The energy in our earlier nonanalytic model[44] yielded -44 kJ/mol and a slightly better agreement with the diffraction experiment.

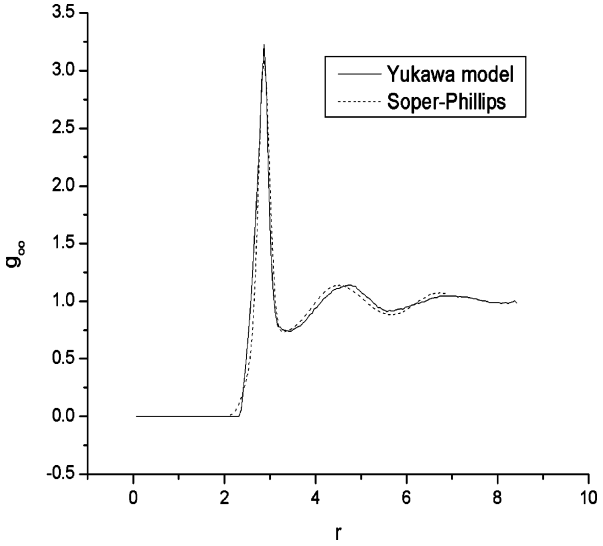

Figure 6. Oxygen−oxygen pair correlation function.

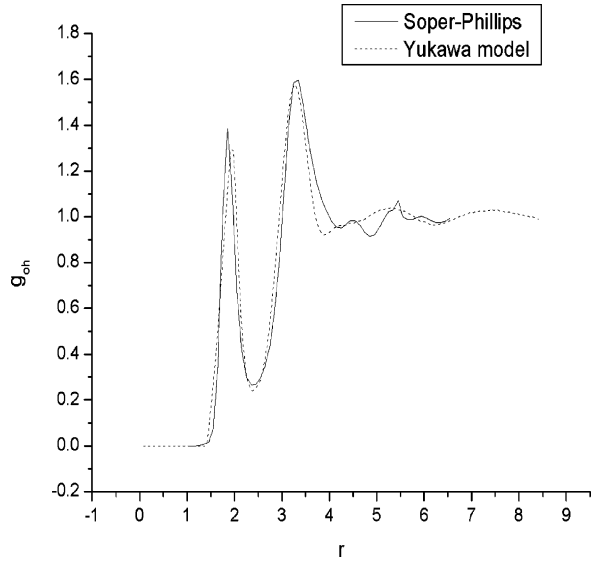

Figure 7. Hydrogen−oxygen pair correlation function.

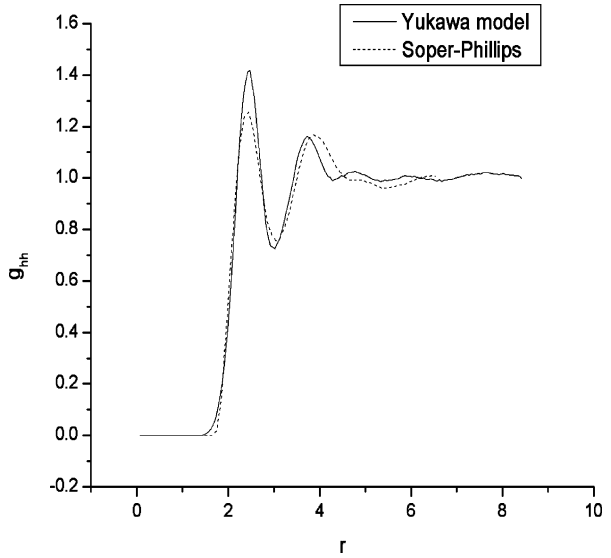

Figure 8. Hydrogen−hydrogen pair correlation function.

Other physical properties of water, such as diffusion coefficients and dielectric properties, are well-reproduced by this model.[66,67]

3. Elementary Processes of the Reaction

The elementary processes of our electrode reaction are driven by the turning of the water molecules in the inner Helmholtz layer. We consider the following steps:

- The reorientation of the water molecules in the inner Helmholtz layer;
- The adsorption and desorption of the bisulfate ions;
- The phase transition that leads to the formation of the 2-dimensional ice, which is the HER compound;
- The desorption of the bisulfate, which originates the "wing" of Clavilier's butterfly; and
- The reversible charge−discharge of the HER compound.

$$[(H_5O_2)^+]_3 + 6e^- \rightleftharpoons 6H + [(H_3O_2)^-]_3 \tag{30}$$

3.1. Reorientation of the Water Molecules in the Inner Helmholtz Layer. In a simple but correct model (for large fields) the turning of the water molecule is done by the interaction of the dipole with the local electric field. Actually, a very simple model of hard polarizable dipoles does exceedingly well in explaining the dielectric properties of water.[68] For positive electrodes, the oxygen points down and binds to the electrode metal atoms. This is so because the strong electric field E will orient the large dipole of the water molecule. The preferred position at positive potential bias is that of an inverted tripod, with the two hydrogen atoms pointing upward. The fugacity of the "oriented" water can be written as

$$z_w = \lambda_W^0 \rho_W^0 g_d^W \tag{31}$$

where $\rho_W^0 = 3.345$ Å^{-3} is the density of water. The water adsorption parameter λ_W^0 is

$$\lambda_W^0 - \exp\{\beta\mu_W E_z(\Delta_\psi)\} \tag{32}$$

with

$$\Delta_\psi \equiv \psi - \psi^{Me} = \Delta\psi = 38.94\Delta\phi \text{ (Volts)}$$

g_d^W is the orientation parameter of the water molecules in contact with the electrode. We use the EXP approximation[59] to get the perpendicular component of the electric field, $E_z(\Delta_\psi)$, at contact with the electrode. The resulting expressions are asymptotically accurate for the contact probabilities because this approximation satisfies the sum rules for the contact densities,[69−72] as was discussed previously.

$$E_z(\Delta_\psi) = -\frac{\kappa}{\beta e}\sinh(\Delta\psi/2) \tag{33}$$

where κ is the Debye−Hueckel parameter, β is the inverse temperature, and e is the electron charge. From here, we compute the polarization of the first layer. The major contribution to the electrostatic energy in our water model is the dipole term, then we can make a simple but asymptotically correct estimate of the orientation parameter of the water molecules near the charged electrode, which can be obtained using the exponential approximation[59] which consists of taking the exponential of the contact mean spherical value.[73−75]

$$g_d^W = -\frac{\sqrt{3}\beta\mu_W E_z(\Delta\psi_W)}{\lambda(2+\lambda)}\exp\{-(1/4)(\lambda+1)\Gamma\sigma\} \tag{34}$$

This relation is exact in the high coupling−low concentration limit.[76,77] The parameters in this equation are Γ, the MSA screening length; μ_W, the dipole moment of water; and σ, the diameter of the water molecule (2.8 Å). The polarization parameter, λ, is the MSA Wertheim parameter, obtained from the eq

$$4\sqrt{\epsilon_W} = \lambda(1+\lambda) \tag{35}$$

where ϵ_W is the bulk dielectric constant of pure water (78.4 at 298 °K), for which we get

$$\lambda = 2.653$$

From these, we get for the dipolar approximation

$$g_d^W = \frac{2\sqrt{3}\kappa\mu_W}{e\lambda(2+\lambda)}\sinh(\Delta\psi_W/2)\exp\{-(1/4)(\lambda+1)\Gamma\sigma\} \tag{36}$$

$$= 0.0943\sinh(19.46\Delta\sigma_W)\exp\{-2.4635\Gamma\sigma\} \tag{37}$$

which is used in conjunction with eq 11 to compute the average orientation of the water molecules.

The above calculation is based on very recent results for what we call the EMSAP approximation,[78] applied to a smooth electrode with a discrete solvent at a finite applied potential.[75] In this theory, the properties (structure and thermodynamics) of a fluid are given in terms of a matrix of scaling parameters **Γ**, which are an extension of the Γ parameter of the MSA for an ionic solution.

The capacitive current due to the flipping of the water molecules is computed from the orientational fugacity z_W as defined in eq 31, and also eqs 36 and 37

$$\theta_W \simeq \frac{2}{5}\left[\frac{\alpha z_W \exp\{K_s\}}{1+\alpha z_W \exp\{K_s\}}\right] \tag{38}$$

where α is an adjustable constant that determines the position of the maximum of the voltammogram in region 3. The main point here is that water is coadsorbed with bisulfate, which will occupy three-fifths of the available water adsorption sites. Since in the tripod adsorption geometry, three oxygen atoms are bound to the Pt substrate, this corresponds to a one-fifth coverage of

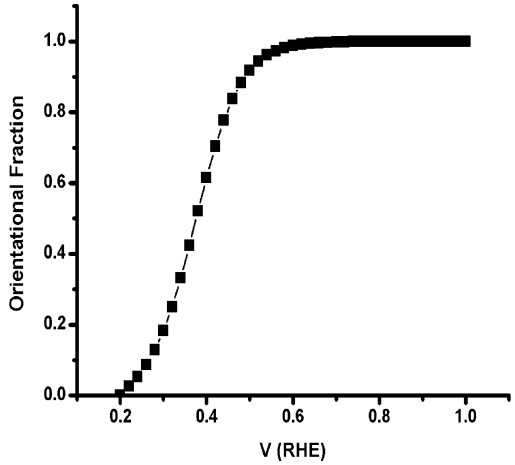

Figure 9. Orientational order parameter. The position of the "turning point", where one-half of the water molecules are oriented either way, is ~0.4 V(RHE) in this graph.

bisulfate, in agreement with experiment[18] and other previous evidence.[52] The correct asymptotic behavior for positive electrodes is exhibited by this isotherm. This equation is obtained from an Ising-type lattice model obtained with the assumption that the straightness of the pattern of elongated hexagons depends on the fugacity of the sulfate and, hence, the constant K_S. In Figure 9, we show the change of θ_W with the applied potential.

The change in the orientation of the water molecules will produce a change in the capacitive current density

$$j_c = (1/A)\left[C + \psi\frac{dC}{d\psi}\right]\frac{d\psi}{dt} \propto (M/A)e\zeta\frac{d\theta_W}{d\psi}\frac{d\psi}{dt} \qquad (39)$$

where C is the integral capacitance; M/A is the number of adsorption sites per area; e is the elementary charge; and ζ is a partial charge of the adsorbate, which we take as 1.

The parameter α determines the position of the maximum of the reorientation current and was adjusted in our previous work[3-6] to ~0.7 V to explain the feature in region 3 of the voltammogram. A much better choice is to take a value close to the thermodynamic point of zero charge (pzc), which has been recently measured experimentally.[27] Without getting into the subtleties of the definition of the pzc, we should remark that the pzc is an average parameter of the entire double layer (including the metal electrode), whereas we are interested in the orientation of the first monolayer of water only. These parameters correspond to different physical situations..

3.2. Adsorption and Desorption of the Bisulfate Ions. The inner layer equivalent fugacity z_S for the adsorption of the bisulfate is

$$z_S = \lambda_S^0\rho_S^0(0, 0)\exp\{-\zeta_S\beta e(\psi - \psi_S^{Re})\exp\{K_S\}\} \quad (40)$$

where $\beta = 1/kT$ is the Boltzmann thermal factor, the electrosorption valency of the bisulfate is $\zeta_S = -1$, and ψ_S^{Re} is the electrosorption reference potential that depends on the nature of the substrate. The sticking coefficient can be interpreted as $\lambda_S(\psi) = \exp(\beta\mu_S)$, with μ_S as the binding free energy of the bisulfate ion to the metal surface. $\rho_S^0(0, \psi)$ is the inner layer local density of bisulfate for a local potential, ψ, which is estimated from the Gouy-Chapman formula.

$$z_S = \lambda_S^0\rho_S^0(0, 0)\exp\{\beta e(\psi - \psi_S^{Me})\} = z_S^0\exp\{\beta e(\psi - \psi_S^{pzc})\} \quad (41)$$

where we take

$$\psi_S^{pzc} = 0.5\ V\ (\text{RHE}) \qquad (42)$$

The adsorption isotherm for bisulfate in region 3 is

$$\theta_S \simeq \frac{1}{5}\left[\frac{z_S}{1 + z_S}\right] \qquad (43)$$

which is asymptotically correct for large positive potentials.

The bisulfate fugacity, z_S, is ($z_S^0 = 1$, $T = 298.16$ K)

$$z_S = \exp\{38.922[\psi - \psi_S^{pzc}]\} \qquad (44)$$

The electrovalence is taken as $\zeta_S = -1$.

3.2.1. The Elongated Hexagon Phase. In much of the ex situ and in situ literature of water adsorption in which water hydrogen bonded structures are shown, they are always pictured as straight O-H-O moeties. To keep this geometry, the water dipoles need to alternate; however,[37] because of the rather large fields and field gradients at the electrode surface, the water dipole is either oriented with the dipole up or down, according to the field. Alternating dipoles are possible only in the immediate neighborhood of the point of zero charge.

There is another problem with the alternating model. The O-Pt distance would also alternate between a close distance of something like 2 Å for the "lower" water molecule to about 3 Å for the "upper" water molecule. It is hard to imagine that the Pt-O bond can stretch that much without breaking. This means that only every other water molecule is attached to the Pt, and it would be hard to understand the very perfect alignment of the extended hexagons seen in the STM pictures. For this reason, we propose another model, which is consistent with the flipping of the dipoles and in which all the water molecules are adsorbed at the same distance from the metal. The single hydrogen bond is displayed in Figure 4, and the chain in Figure 10. It is clear also that at every water, the chain has two possible directions to go, which form an angle of 120°. It is the bisulfate that prevents this from happening. For low bisulfate concentration, a large number of these kinks should be observed.

The STM structures seen in these systems in the positive end of the voltammogram by various authors[28,30,31] consist of elongated hexagons, which are either, as shown in Figure 11, $\sqrt{3} \times \sqrt{7}$ or $\sqrt{3} \times 2.5$, R90, as in Figure 12 Both correspond to a coverage of bisulfate of $\theta = 1/5$. The difference in the S-S distance is <2.50 Å for Figure 11 and 2.64 Å for Figure 12.

The elongated structures corresponding to water coadsorption, as was shown by Ito,[32,33] have been interpreted as being the result of hydrogen bonded water chains. The model we are proposing has a bent hydrogen bond, shown in Figure 3. The O-H-O angle here is 141°.This structure of the hydrogen bond also occurs in the HER compound, where a detailed quantum mechanics calculation shows that there are two angles, 156° and 161°, as shown in Figure 16. The formation of water hydrogen bonded chains occurs because the properly oriented water molecules form hydrogen bonds with the lone pair and one of the two hydrogen atoms of the "upper" plane. In principle, any of the two can form the next bond, and therefore, the "water chain" chain will consist of units forming an angle of 142° to 152°(see Figure 3), instead of the straight 180°, and the "free" hydrogen will be pointing to either side of the chain. If consecutive free hydrogen atoms point to opposite sides of the chain, then the space between next nearest neighbors can be occupied by a bisulfate ion.

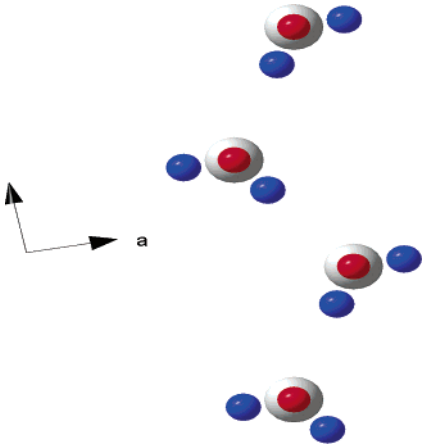

Figure 10. Structure of the hydrogen bonded water chain on a Pt-(111) surface: The small spheres are the oxygen atoms sitting atop the larger Pt atoms. The hydrogen atoms are the darker spheres. One forms a hydrogen bond with its neighbor, and the other forms a bond with the adsorbed bisulfate ion.

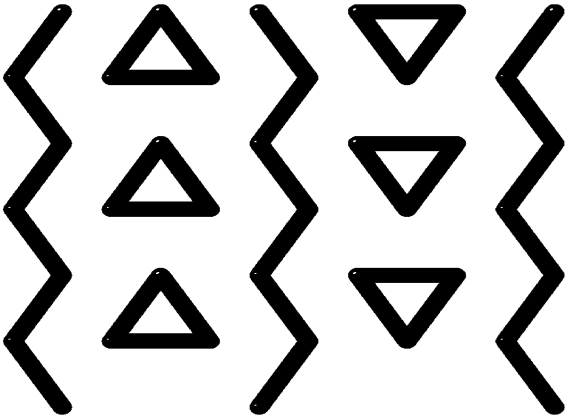

Figure 11. $\sqrt{3} \times (5/2)R$ 90° structure: The triangles are bisulfate ions and the zigzag line are the hydrogen bonded water molecules.

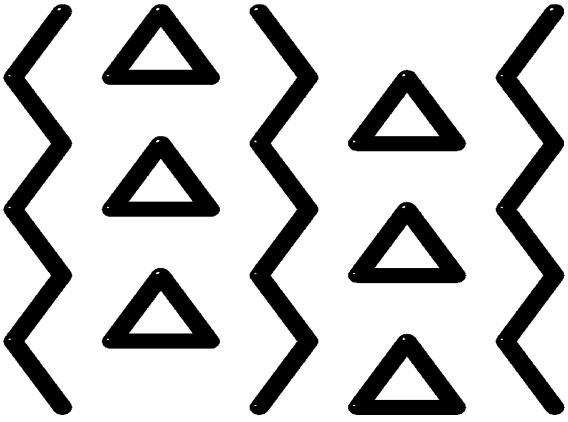

Figure 12. $\sqrt{3} \times \sqrt{7}$ structure: The triangles are bisulfate ions, and the zigzag line is the hydrogen bonded water molecules. Water chain structure, viewed from above. Same as Figure 11, but the bisulfates are all oriented the same way. The structure is now $\sqrt{3} \times \sqrt{7}$, in which the sulfur to sulfur distance is 2.64 Angstrom.

3.3 Formation of the 2-Dimensional Ice. The main point of our theory is the formation of a hexagonal, two-dimensional honeycomb, two-dimensional "ice" structure, shown in Figure 13 which corresponds to the spike of the Clavilier papillon (CP, region 2 in Figure 1). The chemical reaction is as follows:

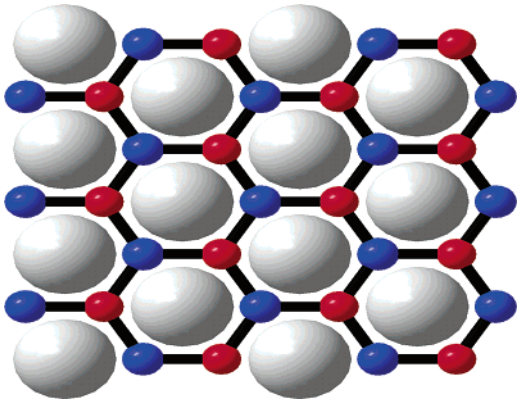

Figure 13. The honeycomb bisulfate−water−hydronium lattice. It is commensurate with the adsorption sites of the Pt(111) face. The hexagons have three water molecules and three hydronium ions in alternating positions. The big spheres at the center of the hexagons represent the bisulfate ions, which eventually are desorbed, leaving the HER structure intact.

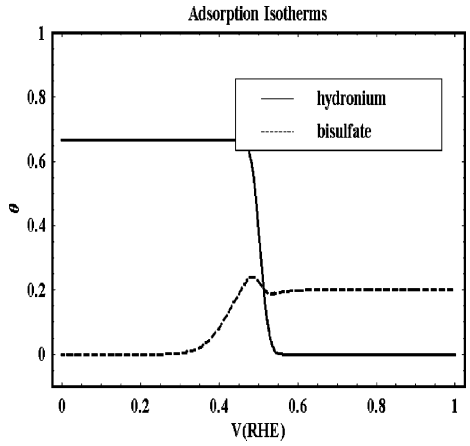

Figure 14. WH−bisulfate coadsorption transition coverages.

$$\underset{\text{elongated hexagons}}{\frac{1}{5}SO_4H^- + \frac{2}{5}H_2O} \rightarrow \underset{\text{2D ice lattice}}{\frac{1}{3}SO_4H^- = \frac{1}{3}H_2O + \frac{1}{3}H_3O^+} \quad (45)$$

The "wing" of the CP[16−18] is associated with the desorption of (bi)sulfate and corresponds also in our theory to the desorption of the bisulfate. In the HER intermediate, the water−hydronium honeycomb lattice stays intact. Since the bisulfate−bisulfate interaction is likely to be very weak (no hydrogen bonding to the HER), we neglect it and use the Langmuir adsorption isotherm.

The CO displacement experiments of Feliu and co-workers[20,21] show very clearly that the one-third corresponding to the "wing" of the butterfly is capacitive and is due to the desorption of the bisulfate, which is what we propose in our theory. Input parameters are the fugacity of "up" water (W), the fugacity of "up" hydronium (H), and that of the bisulfate (S). The formation of the honeycomb structure requires an equimolecular mixture of W and H. The asymptotic occupancy is 1/3 for W, 1/3 for H, and 1/3 for S. In the ideal case at the transition, the coverage of bisulfate goes from one-fifth to one-third

$$\Delta\theta_S = 1/3 - 1/5 = \frac{2}{15} = 0.133 \quad (46)$$

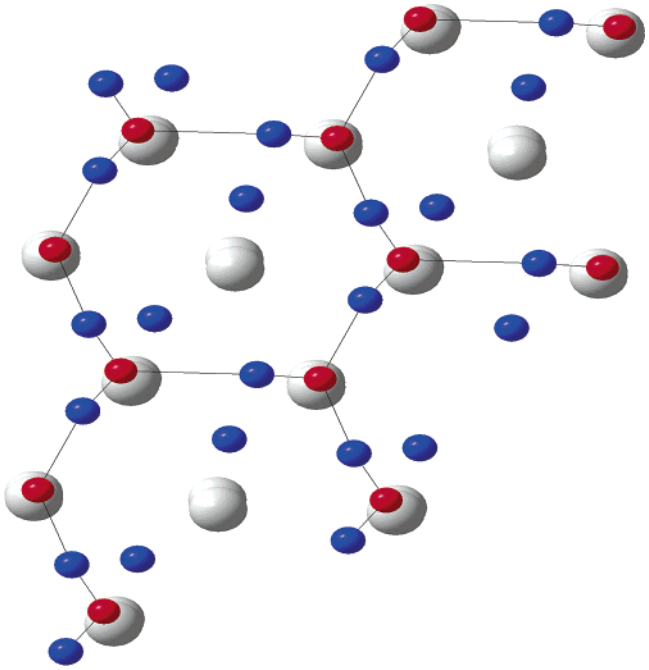

Figure 15. HER honeycomb compound viewed from above. The smaller oxygen atoms are almost on top of the platinums. The centers of the hexagons are not occupied.

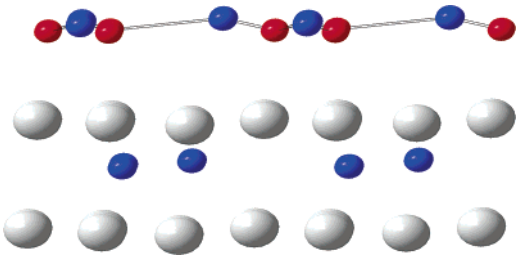

Figure 16. Side view of the HER honeycomb compound. The top layer is the $(H_3O_2^-)_3$. The next layer is the top Pt atoms layer. Next and just below, we have a layer of H atoms. The bottom layer of Pt is also shown.

As the potential gets more negative, the bisulfate S is completely desorbed, leaving the stable HER honeycomb compound behind so that in our theory, $\theta_S = 1/3$ for a small period, shown as a glitch in Figure 13. The relevant parameters are the S−S interactions, the WH−WH═W−H interactions, and the WH−S interactions.

3.4. Desorption of the Bisulfate Originates the "Wing" of Clavilier's Butterfly. The results of the ACVM (asymptotic cluster variation method) are a series of sharp and soft transitions.[58] In our case, there is only one sharp transition, which corresponds to the coadsorption of bisulfate and hydronium. For simplicity, the adsorption isotherms are represented by smoothened step functions. For the bisulfate,

$$\theta_S = \frac{1}{6}\{1 + \mathrm{Erf}[\Delta_S(\psi - \psi_S)]\} + \frac{1}{15}\{-1 + \mathrm{Erf}[-\Delta_{WH}(\psi - \psi_{WH})]\} \quad (47)$$

and for the WH complex

$$\theta_{WH} = \frac{1}{3}\{1 + \mathrm{Erf}[-\Delta_{WH}(\psi - \psi_{WH})]\} \quad (48)$$

The positions and widths of the transitions are treated as adjustable parameters which, however, correspond to the well-defined physical parameters, such as the size distribution of the surface crystallytes: $\Delta_{WH} = 40$ is the semihydronium transition width, and $\psi_{WH} = 0.5041$ is the position of the semihydronium transition, which occurs when there is simultaneous coadsorption of bisulfate and semihydronium.

$\Delta_S = 12$ is the sulfate; $\psi_S = 0.44$ is the position of the sulfate transition, which is determined by the bisulfate−bisulfate repulsive interaction.

The bisulfate goes from a coverage of one-fifth to one-third, and the semihydronium from zero to two-thirds. The exact values for the bisulfate coverages will depend on the other interaction parameters, and will be discussed in a more detailed ACVM analysis. The coverage for semihydronium are fixed by the experimental hydrogen yield.

3.5. Reversible Charge−Discharge of the HER Compound. Quantum Calculations. High-accuracy quantum-mechanical[6] calculations on this model using the generalized gradient approximation PW91,[79] as implemented in the PWSCF package of Baroni et al.,[80] as well a recent extension of the Car−Parrinello[46] algorithm to ensemble density functional theory were developed by two of us.[81] For technical reasons, neutral systems are required. For that reason, we studied the reaction

$$3(H_5O_2) + 3Pt^0 = 6H^0 + 3(H_3O_2)^- + 3Pt^+ \quad (49)$$

to mimic the gradual discharge of the honeycomb compound from ~0.3 to 0.0V (RHE). The fully relaxed structure forms a honeycomb compound, which is stable for alkaline solutions, while the H is either sucked up by the platinum in the hollow positions or released (as gas), depending on the initial conditions of the calculation. The resulting structure is shown in Figures 15 and 16. In our simulations, the electronic ground state is calculated using density functional theory together with the generalized gradient approximation to the exchange-correlation energy functional. This combines the merit of high structural and thermodynamic accuracy with favorable scaling in the system size. We use periodic-boundary conditions, with a fine sampling of the reciprocal space Brillouin zone, and accurate smearing methods to deal with the discontinuities introduced by the existence of a Fermi surface for the metal. The ions are described via ultrasoft Vanderbilt[82] pseudopotentials, allowing for a manageable number of elements in our plane-wave basis set.

The calculation is done in the absence of electric field and electrolytes, but it is clear that the final state of the model corresponds to 0.0 V in Figure 1. In Figures 15 and 16, we show the results for a fully relaxed calculation in which the initial configuration was that of the HER, $(H_5O_2)_3$. The hydrogen atoms not participating in the hydrogen bonded network were placed in the hollow position of the Pt(111) surface, and consequently, the oxygen is also in that position. As the system relaxes, the lower hydrogen atoms diffuse away from the surface, leaving behind the negatively charged quite planar hexagonal honeycomb structure, which is displayed in Figure 15. While the hydrogen is being detached from the oxygen, the most favorable adsorption position for the oxygen shifts to on top of the platinum position. As we can see in Figure 16, the hydrogen atoms are well-separated from the oxygen but are not exactly below the oxygen.

4. The Voltammogram

The results of the treatment for the adsorption isotherms are shown in Figures 17 and 18. The contributions of the water

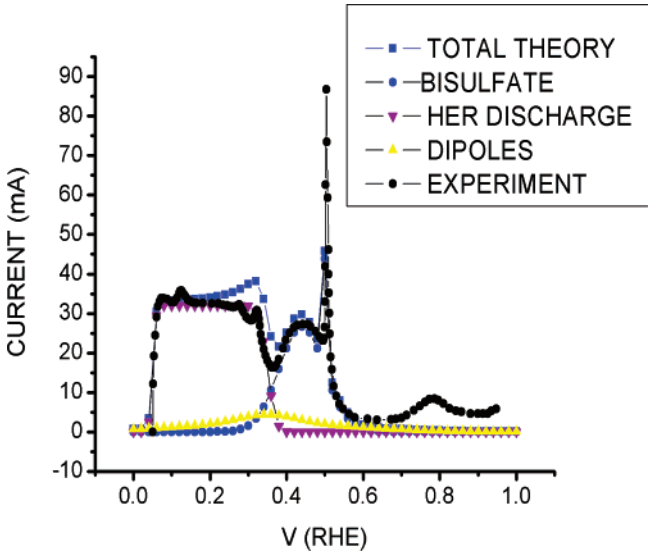

Figure 17. Contributions to the voltammogram and comparison to experiment. The turning point, "PZC", was assumed to be 0.35 V RHE.

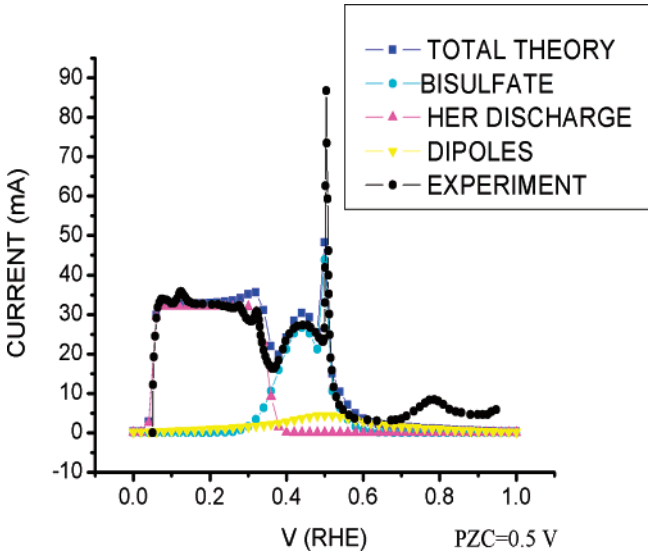

Figure 18. Contributions to the voltammogram and comparison to experiment. The turning point, "PZC", was assumed to be 0.5 V RHE.

dipole reorientation, the phase transition, the desorption of the bisulfate, and the discharge of the HER compound are shown, as well as the comparison to experiment.[27] We have used two different values of α (eq 38): one taken directly from ref 27 for which the E(pzc) is 0.35 V and also 0.5 V. All the other parameters are identical to those of our earlier work.

Our HER model is a hydrogen bonded network of hexagonal rings, which is a form of two-dimensional ice. The chemical formula for a species is

$$[(H_5O_2)^+]_3 \tag{50}$$

and forms a network of hexagonal rings. The explicit reaction taking place at the (111) face of the electrode is

$$[(H_5O_2)^+]_3 + 6e^- = 6H + [(H_3O_2)^-]_3 \tag{51}$$

where the six hydrogen ions that are neutralized are those "trapped" in the hollow sites of the Pt(111) surface.

We assume that a "surface state" is formed by the HER intermediate that discharges linearly with potential. This explains the two-thirds yield for the (111) face in a very natural way. The contribution to the current density of this region is only faradaic.

$$j_F = (M/A)e\left[(\nu - \zeta)\frac{d\theta}{d\psi} - \theta\frac{d\zeta}{d\psi}\right]\frac{d\psi}{dt} \tag{52}$$

where M is the number of adsorption sites per area A, e is the elementary charge, ν is the electrovalence of the adsorbate in the bulk, ζ is the partial charge of the adsorbate at the surface, and ψ is the potential. $(\nu - \zeta)$ is the charge per adsorbate transferred to the surface. The width of the phase transformation and the position of the inflections of g_W and θ_S curves are the only adjustable parameters. There is no adjusting in the total charges.

Figures 17 and 18 show the agreement with experiment for a 0.1 M sulfuric acid solution. Except for region 3, which is now unexplained, the general agreement is good for Figure 17 and much better for Figure 18. The value of 0.5 V seems to us much more natural, since it clearly indicates that water is oriented one way in region 3 and the opposite in regions 1 and 2.

5. Final Comments

The main points in our work are that the tetrahedral geometry of the water potential and the large dipole create two different water "phases" for positively and negatively charged electrodes: long chains at positive potentials and a honeycomb lattice for negative potentials. The formation of the honeycomb two-dimensional ice phase is promoted by the bisulfate or by other anions present, and the spike observed experimentally corresponds to this coadsorption. The honeycomb structure remains in place after the bisulfate has left and is responsible for the two-thirds hydrogen yield of the Pt(111) face. The practical implications of our model will be discussed in future work. We leave the explanation of the features in region 3 for the future.

Acknowledgment. This research was supported by the Office of Energy Research of the U.S. Department of Enegy under Grant DE-FG02-03ER 15422. Useful discussions with J.M. Orts and V. Climent are acknowledged.

References and Notes

(1) Clavilier, J.; Faure, R.; Guinet, G.; Durand, R. *J. Electroanal. Chem.* **1980**, *107*, 205.
(2) Clavilier, J. *J. Electroanal. Chem.* **1980**, *107*, 211.
(3) Blum, L.; Huckaby, D. A. A Phase Transition Induced by Water Reorientation at Electrode Interfaces. In *New Kinds of Phase Transitions: Transformations in Disordered Substances*; Brazhkin, V. V, Buldyrev, S. V., Ryzhov, V. N., Stanley, H. E., Eds.; Proc. NATO Advanced Research Workshop, Volga River, May 2001; Kluwer: Dordrecht, **2002**, p 131.
(4) Blum, L.; Huckaby, D. A. *Mol. Phys.* **2002**, *100*, 2911.
(5) Marzari, N.; Blum, L.; Car, R. The Electroreduction of Hydrogen on Pt(111). *Comput. Nanosci. Nanotechnol. 2002*, **2002**, p 334; www.cr.org.
(6) Blum, L.; Huckaby, D. A..; Marzari, N.; Car, R. *J. Electroanal. Chem.* **2002**, *537*, 7.
(7) Motoo, S.; Furuya, N. *J. Electroanal. Chem.* **1984**, *172*, 339.
(8) Wagner, F. T.; Ross, P. N., Jr. *J. Electroanal. Chem.* **1988**, *250*, 301.
(9) Peremans, A.; Tadjeddine, A. *Phys. Rev. Lett.* **1994**, *73*, 3010.
(10) Nishihara, C.; Nozoye, T. *J. Electroanal. Chem.* **1994**, *379*, 527.
(11) Gomez, R.; Feliu, J. M.; Aldaz, A. *Electrochim. Acta* 1997, *19* (42), 1675.
(12) Gomez, R.; Fernandez-Vega, A.; Feliu, J. M.; Aldaz, A. *J. Phys. Chem.* **1993**, *97*, 4769.
(13) Clavilier, J.; Albalat, R.; Gomez, R.; Orts, J. M.; Feliu, J. M.; Aldaz, A. *J. Electroanal. Chem.* **1992**, *330*, 489.
(14) Zolfaghari, A.; Jerkiewicz, G. *J. Electroanal. Chem.* **1997**, *420*, 11.

(15) Zolfaghari, A.; Jerkiewicz, G. *J. Electroanal. Chem.* **1997**, *422*, 1.
(16) Kunimatsu, K.; Samant, M. G.; Seki, H. *J. Electroanal. Chem.* **1989**, *272*', 185.
(17) Faguy, P. W.; Markovic, N.; Fierro, C. A.; Yeager, E. B. *J. Electroanal. Chem.*, **1990**, *289*, 245.
(18) Kolics, A.; Wieckowsky, A. *J. Phys. Chem.* **2001**, *103B*, 3556.
(19) Koper, M. T. M.; Lukkien, J. J. *J. Electroanal. Chem.* **2000**, *485*, 161.
(20) Feliu, J. M.; Orts, J. M.; Gomez, R.; Aldaz, A.; Clavilier, J. *J. Electroanal. Chem.* **1994**, *372*, 265.
(21) Alvarez, V.; Climent, V.; Feliu, J. M.; Aldaz, A. *Electrochem. Commun.* **2000**, *2*, 427.
(22) Bewick, A.; Tuxford, A. M. *Electroanal. Interface Electrochem.* **1973**, *47*, 255.
(23) Bewick, A.; Kunimatsu, K.; Robinson, J.; Russell, J. W. *J. Electroanal. Chem.* **1981**, *119*, 175.
(24) Bewick, A.; Russell, J. W. *J. Electroanal. Chem.* **1982**, *132*, 329.
(25) Faguy, P. W.; Marinkovic, N. S.; Adzic, R. R. *Langmuir* **1996**, *12*, 243.
(26) Faguy, P. W.; Marinkovic, N. S.; Adzic, R. R. *J. Electroanal. Chem.* **1996**, *407*, 209.
(27) Climent, V.; Coles, B. A.; Compton, R. G. *J. Phys. Chem.* **2002**, *106B*, 5988.
(28) Futnikov, A. M.; Linke, U.; Stimming, U.; Vogel, R. *Surf. Sci.* **1995**, *324*, L343.
(29) Wan, L. J.; Yau, S. L.; Itaya, K. *J. Phys. Chem.* **1995**, *99*, 9507.
(30) Wan, L. J.; Suzuki, T.; Sashikata, K.; Okada, J.; Inukai, J.; Itaya, K. *J. Electroanal. Chem.* **2000**, *461*, 26.
(31) Kim, J. G.; Soriaga, J. B.; Vigh, G.; Soriaga, M. P. *J. Colloid Interface Sci.* **2000**, *15*, 26.
(32) Ogasawara, H.; Sawatari, Y.; Inukai, J.; Ito, M. *J. Electroanal. Chem.* **1993**, *358*, 337.
(33) Sawatari, Y.; Sueoka, A. T.; Shingaya, Y.; Ito, M. *Spectrochim. Acta* **1994**, *50A*, 1555.
(34) Shingaya, Y.; Ito, M. *Interfacial Electrochemistry: Theory, Experiment and Applications*; Wieckowsky, A. Ed.; M. Dekker: New York 1999, p 17.
(35) Coniglio, A.; Fierro, A.; Nicodemi, M. The inherent states of glassy systems and granular media. In *New Kinds of Phase Transitions: Transformations in Disordered Substances*, Brazhkin, V. V., Buldyrev, S. V., Ryzhov, V. N., Stanley, H. E., Eds.; *Proc. NATO Adv. Res. Workshop, Volga River*, Kluwer: Dordrecht, 2002; p 75.
(36) Chidambaram, R. *Acta Crystallogr.* **1961**, *14*, 467.
(37) Mott, N. F.; Watts-Tobin, J. *Electrochim. Acta* **1961**, *4*, 79.
(38) Weissmann, M.; Blum, L. *Trans. Faraday Soc.* **1968**, *64* 2605.
(39) Ben Naim, A.; Stillinger, F. H. *J. Chem. Phys.* **1969**, *51*, 900.
(40) Berendsen, H. J. C.; Grigera, J. R.; Straatsma, T. P. *J. Phys. Chem.* **1987**, *91*, 6269.
(41) Jorgensen, W. L. *J. Am. Chem. Soc.* **1978**, *100*, 7824; **1981**, *103*, 335; *J. Chem. Phys.* **1982**, *77*, 335; **1982**, *77*, 4156.
(42) Blum, L.; Narten, A. H. *Adv. Chem. Phys.* **1976**, *34* 203.
(43) Bratko, D.; Blum, L.; Luzar, A. *J. Chem. Phys.* **1985**, *83*, 6367.
(44) Degreve, L.; Blum, L. *Physica* **1996**, *A 224*, 550.
(45) Blum, L.; Degreve, L.; *Physica* **1999**, *A 265*, 396.
(46) Car, R.; Parrinello, M. *Phys. Rev. Lett.* **1985**, *85*, 2471.
(47) Huckaby, D. A.; Blum, L. *J. Chem. Phys.* **1990**, *92*, 2646.
(48) Blum, L.; Huckaby, D. A. *J. Chem. Phys.* **1991**, *94*, 6887.
(49) Blum, L.; Legault, M. D.; Huckaby, D. A. In *Interfacial Electrochemistry: Theory, Experiment and Applications*; Wieckowsky, A., Ed.; M. Dekker: New York, 1999; p 19.
(50) Huckaby, D. A.; Blum, L. *J. Electroanal. Chem.* **1991**, *315*, 255.
(51) Huckaby, D. A.; Blum, L. *Proc. Electrochem. Soc.* **1993**, *95*−*3*, 232; In *Microscopic Models of Electrode/Electrolyte Interfaces*, Halley, J. W., Blum, L., Eds.
(52) Blum, L.; Huckaby, D. A. *J. Electroanal. Chem.* **1994**, *375*, 69.
(53) Toney, M. F.; Howard, J. F.; Richer, J.; Borges, G. L.; Gordon, J. G.; Melroy, O. R.; Yee, D.; Sorensen, L. B. *Phys. Rev. Lett.* **1995**, *72*, 4472.
(54) Rosinberg, M. L.; Lebowitz, J. L.; Blum, L. *J. Stat. Phys.* **1986**, *44*, 153.
(55) Guggenheim, E. A.; McGlashan, M. C. *Proc. R. Soc. London* **1951**, *206*, 335.
(56) Bell, G. M. *J. Phys. C* **1972**, *5*, 889.
(57) Shinmi, M.; Huckaby, D. A. *J. Chem. Phys.* **1986**, *84*, 951.
(58) Huckaby, D. A.; Legault, M. D.; Blum, L. *J. Chem. Phys.* **1988**, *109*, 3600.
(59) Bernard, O.; Blum, L. *J. Chem. Phys.* **1996**, *104*, 4746.
(60) Simonin, J. P.; Bernard, O.; Blum, L. *J. Phys. Chem.* **1999**, *B 103*, 699.
(61) Blum, L.; Legault, M.; Turq, P. *J. Electroanal. Chem.* **1994**, *379*, 35.
(62) Blum, L.; Torruella, A. J. *J. Chem. Phys.* **1972**, *56*, 303.
(63) Blum, L. *J. Comput. Phys.* **1971**, *7*, 592.
(64) Soper, A. K.; Phillips, M. G. *Chem. Phys.* **1986**, *107*, 47.
(65) Blum, L.; Vericat, F.; Bratko, D. *J. Chem. Phys.* **1995**, *102*, 1461.
(66) Liu, Y.; Ichiye, T. *Chem. Phys. Lett.* **1994**, *231*, 380.
(67) Liu, Y.; Ichiye, T. *Chem. Phys. Lett.* **1996**, *256*, 334.
(68) Blum, L.; Fawcett, W. R. *J. Phys. Chem.* **1993**, *97*, 7 185.
(69) Henderson, D.; Blum, L.; Lebowitz, J. L. *J. Electroanal. Chem.* **1979**, *102*, 315.
(70) Blum, L.; Rasaiah, J. C.; Vericat, F. *J. Chem. Phys.* **1983**, *78*, 3233.
(71) Blum, L. *J. Stat. Phys.* **1994**, *75*, 971.
(72) Blum, L. *Some Exact Results for Coulomb Systems*; Institute of Theoretical Physics, University of California, Santa Barbara CA; http://online.kitp.ucsb.edu/online/bio98/blum, 1998.
(73) Blum, L.; Henderson, D. *J. Chem. Phys.* **1981**, *74*, 1902.
(74) Blum, L.; Vericat, F.; Fawcett, W. R. *J. Chem. Phys.* **1992**, *96*, 3039.
(75) Blum, L. *J. Chem. Phys.* **2002**, *117*, 756; Los Alamos Preprint cond-mat/0111086.
(76) Rosenfeld, Y.; Blum, L. *J. Chem. Phys.* **1986**, *85*, 1556.
(77) 7. Velazquez, E. S.; Blum, L. *J. Chem. Phys.* **1999**, *110*, 10931.
(78) Blum, L.; Hernando, J. A. *Condensed Matter Theories*; Hernandez, S., Clark, J. W., Eds.; Nova Publishers: New York 2001; Vol. 16, p 411.
(79) Perdew, J. P. In *Electronic Structures of Solids '91*, Ziesche, P., Eschrig, H., Eds.; Akademie Verlag: Berlin, 1991; p 11.
(80) 0. PWSCF package; Baroni, S.; Dal Corso, S. A.; de Gironcoli, S.; Giannozzi, P. http://www.pwscf.org.
(81) Marzari, N.; Car, R., in preparation.
(82) Vanderbilt, D. *Phys. Rev. B* **1985**, *32*, 8412.